

LETTER TO THE EDITOR

Direct detection of the Enceladus water torus with *Herschel*^{★,★★}

P. Hartogh¹, E. Lellouch², R. Moreno², D. Bockelée-Morvan², N. Biver², T. Cassidy³,
M. Rengel¹, C. Jarchow¹, T. Cavalié⁴, J. Crovisier², F. P. Helmich⁵, and M. Kidger⁶

¹ Max-Planck-Institut für Sonnensystemforschung, Katlenburg-Lindau, Germany
e-mail: hartogh@mps.mpg.de

² LESIA, Observatoire de Paris, 5 place Jules Janssen, 92195 Meudon, France

³ Jet Propulsion Laboratory, California Institute of Technology, Pasadena, CA 91107, USA

⁴ Université de Bordeaux, Observatoire Aquitain des Sciences de l'Univers, CNRS, UMR 5804,
Laboratoire d'Astrophysique de Bordeaux, France

⁵ SRON, Groningen, The Netherlands

⁶ *Herschel* Science Centre, European Space Astronomy Centre, Madrid, Spain

Received 30 May 2011 / Accepted 22 June 2011

ABSTRACT

Cryovolcanic activity near the south pole of Saturn's moon Enceladus produces plumes of H₂O-dominated gases and ice particles, which escape and populate a torus-shaped cloud. Using submillimeter spectroscopy with *Herschel*, we report the direct detection of the Enceladus water vapor torus in four rotational lines of water at 557, 987, 1113, and 1670 GHz, and probe its physical conditions and structure. We determine line-of-sight H₂O column densities of $\sim 4 \times 10^{13}$ cm⁻² near the equatorial plane, with a $\sim 50\,000$ km vertical scale height. The water torus appears to be rotationally cold (e.g. an excitation temperature of 16 K is measured for the 1113 GHz line) but dynamically excited, with non-Keplerian dispersion velocities of ~ 2 km s⁻¹, and appears to be largely shaped by molecular collisions. From estimates of the influx rates of torus material into Saturn and Titan, we infer that Enceladus' activity is likely to be the ultimate source of water in the upper atmosphere of Saturn, but not in Titan's.

Key words. planets and satellites: individual: Saturn – planets and satellites: individual: Enceladus – techniques: spectroscopic – submillimetre: planetary system

1. Introduction

Saturn is immersed in a surprisingly oxygen-rich environment including long-observed OH radicals (Shemansky et al. 1993) and more recently detected atomic O and O-bearing ions (Esposito et al. 2005; Melin et al. 2009; Tokar et al. 2006). Models developed by Jurac et al. (2001, 2005) suggested a large water source near Enceladus' orbit as the main supply of OH, a view later supported by the discovery of active, H₂O-rich plumes near Enceladus' south pole (Porco et al. 2006; Hansen et al. 2006; Waite et al. 2006). Gases and particles escaping from Enceladus vents are expected to form a torus-shaped cloud and populate Saturn's E ring, but except for difficult and low signal-to-noise in situ measurements performed by the Cassini Ion Neutral Mass Spectrometer (INMS; Perry et al. 2010), H₂O itself has not been adequately sampled in Saturn's environment away from Enceladus. In this paper, using submillimetre spectroscopy with the Heterodyne Instrument for the Far-Infrared (HIFI, de Graauw et al. 2010) on the *Herschel* Space Observatory (Pilbratt et al. 2010), we report the direct detection of the H₂O Enceladus torus in absorption against Saturn and its physical characterization.

* *Herschel* is an ESA space observatory with science instruments provided by European-led Principal Investigator consortia and with important participation from NASA. HIFI has been designed and built by a consortium of institutes and university departments from across Europe, Canada and the United States under the leadership of SRON Netherlands Institute for Space Research, Groningen, The Netherlands and with major contributions from Germany, France and the US.

** Figures 4 and 5 are available in electronic form at <http://www.aanda.org>

2. Observations and initial interpretation

Emission lines due to water vapor in the far-infrared spectrum ($\lambda > 30$ μ m) of the giant planets and Titan, first discovered by ISO (Feuchtgruber et al. 1997; Coustenis et al. 1998) prove the existence of an external supply of water to these reducing atmospheres. At Saturn and Jupiter, spectrally resolved observations of the fundamental 1₁₀-1₀₁ line of ortho-H₂O at 557 GHz (538 μ m), obtained by SWAS in September 1999 (Bergin et al. 2000), indicated a $\sim 10\%$ contrast emission with ~ 20 km s⁻¹ width.

Unexpectedly, disk-averaged observations of Saturn with *Herschel*/HIFI performed on June 21 and July 8, 2009, revealed an additional $\sim 20\%$ deep, 6 km s⁻¹-wide absorption in the line core (Fig. 1). A Saturn origin for the absorption can be readily dismissed. First, the brightness temperature in the line core is ~ 90 K, a temperature that does not occur in Saturn's upper atmosphere (e.g. Nagy et al. 2009). Second, even if such a cold layer existed, the negligibly small vapor pressure of water at 90 K ($< 10^{-20}$ bar) would preclude any absorption by H₂O. Finally, the linewidth is too narrow for line formation at Saturn, given the planet's 9.9 km s⁻¹ equatorial rotation velocity. Therefore, the absorption must be produced by material in the foreground.

The striking difference between the SWAS and *Herschel* observations must be related to the different observing geometries, with the ring/satellite system wide being open in 1999 (sub-observer planetocentric latitude $\beta = -21^\circ$) and much more edge-on in 2009 ($\beta = -3^\circ$), suggesting that the absorbing molecules are confined to the equatorial plane. The Enceladus torus, a tenuous ring of material fed by gases escaping from Enceladus'

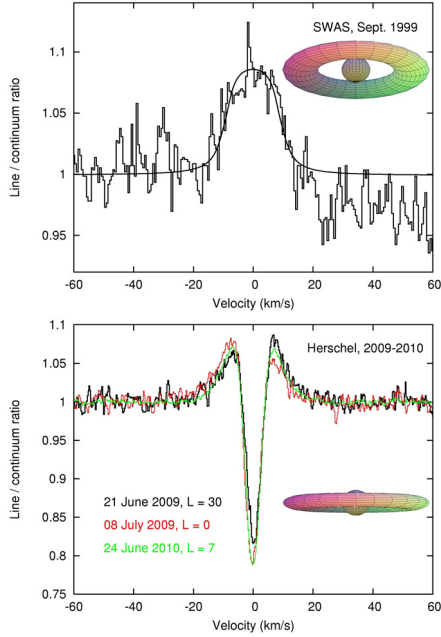


Fig. 1. *Top:* the $1_{10}-1_{01}$ line of H_2O at 556.936 GHz observed by (*top*) SWAS in Sept. 1999 (Bergin et al. 2000). The sub-observer planetocentric latitude is $\beta = -21^\circ$. The $\sim 20 \text{ km s}^{-1}$ emission linewidth is primarily caused by the rapid (9.9 km s^{-1}) rotation of the planet. The solid line is the SWAS-derived model for H_2O in Saturn’s stratosphere. *Bottom:* same line, observed by *Herschel/HIFI* on June 21 and July 8, 2009 ($\beta = -3^\circ$) and June 24, 2010 ($\beta = +2^\circ$). The orbital longitude of Enceladus on these three dates is 30° , 0° , and 7° , respectively (0° corresponds to the sub-Saturn point being visible at disk center). The insets show a rough sketch of the associated torus appearance.

plumes and centered on Enceladus’ orbit near 3.95 Saturn radii (R_S), offers a promising explanation. Although the circular Keplerian orbital velocity at $\sim 4 R_S$ is $\pm 12.6 \text{ km s}^{-1}$, its radial projection for line of sights (LOS) intersecting Saturn is about one quarter of this value, matching the linewidth requirement.

Dedicated observations (Fig. 2), including in addition the $2_{02}-1_{11}$ (987 GHz), $3_{12}-3_{03}$ (1097 GHz), $1_{11}-0_{00}$ (1113 GHz), and $2_{12}-1_{01}$ (1670 GHz) H_2O lines, were obtained on June 24, 2010 ($\beta = +2^\circ$) in the framework of the “HssO” key program (Hartogh et al. 2009). Since the HIFI beam at 1670 GHz (HPBW $\sim 12.6''$) partially resolves Saturn’s $\sim 16.5''$ disk, a crude five-point map (center, east, west, north, south) was also obtained in that line.

3. Excitation and torus models

In a physical situation similar to cometary atmospheres, water molecules in orbit around Saturn are subject to excitation processes caused by the ambient radiation field and possibly collisions. Radiative excitation processes include radiative populating of pure rotational levels as well as IR pumping of vibrational bands followed by radiative decay. We adapted a cometary code (Bockelée-Morvan & Crovisier 1989) to Saturn’s conditions to calculate the populations of the H_2O rotational levels under fluorescence equilibrium, assuming an ortho/para ratio of three. In addition to solar radiation and the 2.7 K cosmic background, we took into account Saturn’s thermal field – described for simplicity as a constant 100 K brightness temperature source at a fixed $4 R_S$ distance. We found that the latter dominates the radiative excitation of rotational levels, while solar radiation prevails for IR pumping. Excitation by $\text{H}_2\text{O}-\text{H}_2\text{O}$ collisions was found to be negligible. On the basis of detailed calculations

following Zakharov et al. (2007), H_2O -electron collisions were also found to be of a minor importance, given the electronic densities and temperatures measured in the torus (Persoon et al. 2009).

Model results indicate that for both the ortho and para states, most of the molecules ($\sim 93\%$) appear to be in the fundamental levels (1_{01} and 0_{00} , respectively), and the next populated levels are the 1_{10} (ortho) and 1_{11} (para) levels, with populations in the model of 0.043 and 0.059 (relative to the fundamental levels). Hence, lines originating in the fundamental levels, i.e. the ortho 557 and 1670 GHz lines and the para 1113 GHz line, are predicted to be strongly absorbed. Weak absorption is expected in the $2_{02}-1_{11}$ para line (987 GHz), while higher energy lines, such as the 1097 GHz line with a 137 cm^{-1} lower energy level, equivalent to 196 K , are expected not to show any detectable absorption. All these predictions agree with observational results (Fig. 2).

Observations were modeled with a simplified, “homogeneous”, torus model. Torus material is characterized by its local number density and local distribution of velocity vectors. The latter is described by the combination of Keplerian velocity and a velocity dispersion V_{rms} . Doppler-shaped line profiles characterized by V_{rms} are calculated and locally Doppler-shifted according to the LOS-projected circular Keplerian velocity. Line profiles are converted into opacity profiles by using the excitation model above. The radial structure of the torus is described by its inner and outer limits, and a constant H_2O number density along each line-of-sight is assumed. Free model parameters are thus the H_2O column density ($N_{\text{H}_2\text{O}}$) and the molecule velocity dispersion V_{rms} , the latter being assumed to be constant throughout the torus. Nominally, the torus is assumed to be centered on the Enceladus orbit at $3.95 R_S$ and to extend from 2.7 to $5.2 R_S$ (i.e. over a $2.5 R_S$ distance; Farmer 2009). Model results for a radially more confined (e.g. a $1.5 R_S$ extension; Cassidy and Johnson 2010) or even an infinitely narrow torus were insignificantly different; in contrast, as discussed below, models are sensitive to the central position of the torus. To model the emission part of the lines, we included the SWAS-derived model for the distribution of H_2O in Saturn’s stratosphere (Bergin et al. 2000), with a water column of $5.5 \times 10^{16} \text{ cm}^{-2}$.

In a first step, $N_{\text{H}_2\text{O}}$ was assumed to be uniform across Saturn’s disk, and in the case of the 1670 GHz map, determined separately for each beam position. Being optically thin, all lines are well suited to a precise determination of the H_2O columns. For the 1670 GHz line, the east and west limb positions have complex line shapes, that are Doppler-shifted and have only one wing absorbed, reflecting the interplay between Saturn’s rotation and the torus orbital velocity. They therefore show good sensitivity to both V_{rms} and the torus location. As shown in Figs. 2 and 4, the best-fit solution is obtained for $V_{\text{rms}} = 2.0-2.3 \text{ km s}^{-1}$ and $N_{\text{H}_2\text{O}} = (1.5-1.75) \times 10^{13} \text{ cm}^{-2}$, and the torus is indeed centered at $\sim 4 R_S$ (and not, for instance, in Saturn’s main rings at $< 2 R_S$). Given its simplicity, the model gives a remarkably good match to most lines. The weak 987 GHz line requires a water column 1.7 ± 0.3 times larger than for other lines, pointing to larger excitation (by the same factor) of the 1_{11} level than predicted by our model. We leave this issue for future work, noting that this does not affect our conclusions about either the torus density or structure, as deduced from the other lines, since $\sim 90\%$ of the molecules are in the fundamental levels. Water still appears to be rotationally cold, as the data imply an excitation temperature of $\sim 16 \text{ K}$ for the $1_{11}-0_{00}$ (1113 GHz) line.

The north pole spectrum at 1670 GHz indicates a factor-of-two lower $N_{\text{H}_2\text{O}}$ than other beam positions, implying that there

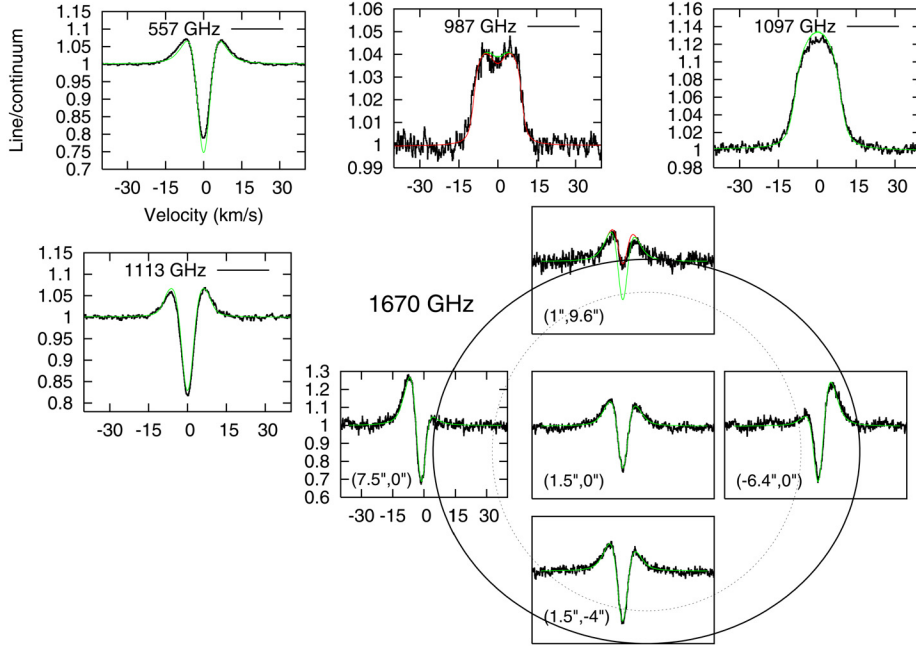


Fig. 2. Entire set of *Herschel* / HIFI H₂O observations of June 24, 2010. Saturn’s sub-observer latitude $\beta = +2^\circ$. The 557, 987, 1097, and 1113 GHz lines were observed sequentially at an orbital longitude of Enceladus $L = 8^\circ\text{--}24^\circ$, while the 1670 GHz map was acquired at $L = 128^\circ\text{--}134^\circ$. Observations are here modeled with a simplified, “homogeneous”, torus model whose free parameters are the H₂O column density ($N_{\text{H}_2\text{O}}$) and the velocity dispersion of the molecules (V_{rms} , assumed constant throughout the torus). Green lines are models with $V_{\text{rms}} = 2.3 \text{ km s}^{-1}$ and $N_{\text{H}_2\text{O}} = 1.5 \times 10^{13} \text{ cm}^{-2}$ ($1.75 \times 10^{13} \text{ cm}^{-2}$ for the 1670 GHz east, west and south limbs spectra). The red line at 987 GHz has $N_{\text{H}_2\text{O}} = 2.5 \times 10^{13} \text{ cm}^{-2}$. The red line for the 1670 GHz north limb spectrum has $N_{\text{H}_2\text{O}} = 0.75 \times 10^{13} \text{ cm}^{-2}$. For the 1670 GHz map, precise pointing (as indicated as RA, Dec offsets from Saturn’s center as inset) was recovered from the examination of the continuum levels and slight line asymmetries. The inner dotted circle compares the 12.6'' beam at this frequency with Saturn $17.2'' \times 15.4''$ disk (outer solid circle).

is some vertical confinement of the torus. Assuming in a second step that $N_{\text{H}_2\text{O}}$ varies as $N(z) = N_{\text{eq}} e^{-z/H}$, where z is the distance from the equatorial plane, and convolving local line profiles by the HIFI beams, we infer an equatorial column density $N_{\text{eq}} = 4^{+2}_{-1} \times 10^{13} \text{ cm}^{-2}$ and a scale-height $H = 0.4^{+0.2}_{-0.1} R_S$ (Fig. 5). This is in sharp contrast to tentative results from the Cassini/INMS (Perry et al. 2010) from which $H \sim 0.05 R_S$ was inferred, based on measurements of CO and H₂ (produced in the instrument from CO₂ and H₂O).

Water emitted from Enceladus’ plumes in jets with $\geq 1 \text{ km s}^{-1}$ velocity (Hansen et al. 2008, 2011) initially forms a narrow torus. However, the observed OH distribution (Melin et al. 2009) requires acceleration and spreading, for which processes identified early on (Jurac & Richardson 2005; Johnson et al. 2006) include the release of kinetic energy under photodissociation and collisions with rapid torus ions. Momentum transfer associated with H₂O-H₂O collisions (“viscous heating”) was first investigated in a fluid model by Farmer (2009) – who actually predicted the observability of the torus with *Herschel*, but in emission. On the basis of a Monte-Carlo model, in which the ejection rate from Enceladus is the only free parameter (nominally $1 \times 10^{28} \text{ s}^{-1}$), Cassidy and Johnson (2010) showed that elastic collisions, mostly in the inner part of the cloud, pump up particle eccentricities to large values (~ 0.5), resulting in additional torus spreading and heating. Their model calculates three-dimensional distributions of velocities and H₂O number densities, hence LOS column densities across Saturn’s disk for any vantage point.

The third step of our analysis therefore consisted of a partial test of this model. For this the model-predicted LOS water columns across Saturn’s disk for the appropriate viewing geometry and as a function of the Enceladus water source rate were used as input to the radiative transfer model. Note that we did not

explicitly incorporate model predictions for the distribution of velocity vectors. Instead, we proceeded with the above approach of constant and adjustable V_{rms} (found to be 2.0–2.3 km s⁻¹). As shown in Fig. 5, a $0.85 \times 10^{28} \text{ s}^{-1}$ Enceladus source rate satisfactorily matches the absolute H₂O column densities and their latitudinal dependence. The maximum (equatorial) LOS water columns are $\sim 4 \times 10^{13} \text{ cm}^{-2}$. The associated water map is shown in Fig. 3 for both the *Herschel* and SWAS geometries. Note that the (number-density-weighted) mean rms velocity in the model relative to circular motion is 1.77 km s⁻¹, slightly below but generally consistent with the 2.0–2.3 km s⁻¹ range inferred from observations. We also ran the physical model with the neutral-neutral collisions “turned-off”, to assess the importance of this processes. In that case, the vertical torus scale height in the model is 0.1–0.15 R_S , and the mean rms velocity is 0.95 km s⁻¹, both of which disagree with the data. Hence, both the measured gas velocities and torus scale-height illuminate the role of neutral-neutral collisions in shaping the torus.

4. Discussion and implications for the source of water in Saturn and Titan

A $0.85 \times 10^{28} \text{ s}^{-1}$ source rate is typical of values inferred from Cassini measurements. Plume variability at the ~ 1 order of magnitude level has been documented based on INMS and magnetic field data (Smith et al. 2010; Saur et al. 2008). In contrast, UVIS occultations (Hansen et al. 2011) indicate a remarkable stability of the source rate, with variations as low as $\sim 15\%$ around a mean $0.7 \times 10^{28} \text{ s}^{-1}$ value. The lifetime of H₂O molecules against photodissociation, ~ 2.5 months (Cassidy & Johnson 2010; Smith et al. 2010) allows variability of the torus on comparable timescales. Remarkably the HIFI data do not

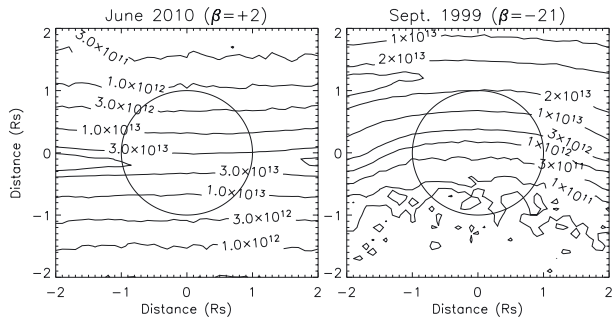


Fig. 3. Model H₂O column density maps for a $0.85 \times 10^{28} \text{ s}^{-1}$ Enceladus source rate, for the *Herschel* ($\beta = +2^\circ$, left) and SWAS ($\beta = -21^\circ$, right) observing geometries, and an orbital longitude of Enceladus $L = 130^\circ$. In the SWAS geometry, the largest line-of-sight columns occur outside of Saturn's disk. The unmarked contours are at $4.5 \times 10^{13} \text{ cm}^{-2}$ in the left panel and 3×10^{13} and $5 \times 10^{10} \text{ cm}^{-2}$ in the right panel.

show evidence of even small variations between June/July 2009 and June 2010, a behavior also reminiscent of the low variations in the global O content in the torus over 2003–2004 (Melin et al. 2009). Although none of the HIFI observations sampled the region near Enceladus itself (orbital longitude $L \sim 180^\circ$), our data do not show any variation with the Enceladus orbital position (Figs. 1 and 2), especially between $L \sim 0^\circ$ – 30° and $L \sim 130^\circ$, demonstrating considerable azimuthal mixing on timescales ($\sim 6 \times 10^5 \text{ s}$) much shorter than the H₂O lifetime.

Beyond the loss to space, the ultimate fate of the H₂O (and other species) emitted from Enceladus vents is to coat the surfaces of the satellites and the main rings (Verbiscer et al. 2007; Hendrix et al. 2010) or to precipitate into Saturn's and Titan's atmospheres (Cassidy & Johnson 2010). For a $0.85 \times 10^{28} \text{ s}^{-1}$ Enceladus source rate, our model indicates a $\sim 2.5 \times 10^{26} \text{ (OH+H}_2\text{O) molec s}^{-1}$ flux into Saturn, i.e. $\sim 6 \times 10^5 \text{ cm}^{-2} \text{ s}^{-1}$. This matches the $(1 \pm 0.5) \times 10^6 \text{ cm}^{-2} \text{ s}^{-1}$ value required to explain Saturn's upper atmosphere water vapor (Moses et al. 2000; Ollivier et al. 2000). Enceladus is thus the likely source of Saturn's external water, though an additional confirmation could be provided by the latitudinal distribution of H₂O on Saturn. As for Titan, the modeled planet-averaged flux is $\sim 1 \times 10^6 \text{ O cm}^{-2} \text{ s}^{-1}$ and $4 \times 10^5 \text{ (OH+H}_2\text{O) cm}^{-2} \text{ s}^{-1}$ referred to the surface, where the higher O flux is due to the broader radial extent of the O torus (Melin et al. 2009; Cassidy & Johnson 2010). Given the external fluxes needed to explain Titan's oxygen compounds ($(1\text{--}4) \times 10^6 \text{ O atom cm}^{-2} \text{ s}^{-1}$ and ~ 2 times more H₂O, see review in Strobel et al. 2009) and the observed plume variability, Enceladus may thus provide adequate O to supply Titan's CO (Hörst et al. 2008), but falls short by a factor ~ 5 – 20 for H₂O.

The nature of the external supply of water into all other outer planet stratospheres has long remained uncertain, potentially including significant contributions from micrometeoroid dust particles, cometary impacts, and local ring/satellite sources. The similar H₂O fluxes per unit area into the four giant planets and Titan (Feuchtgruber et al. 1997; Coustenis et al. 1998; Moses et al. 2000), combined with the rather constant dust flux ($\sim 3 \times 10^{-18} \text{ g cm}^{-2} \text{ s}^{-1}$) measured in interplanetary space beyond 5 AU (Landgraf et al. 2002) have been regarded as evidence that micrometeoroids – interplanetary (IDPs) or interstellar – are the dominant source (Moses et al. 2000). Along with the evidence that the H₂O present in Jupiter's atmosphere results from the Shoemaker-Levy 9 1994 impact (Lellouch et al. 2002) – and that CO in Jupiter, Saturn, and Neptune (Bézar et al. 2002;

Cavalié et al. 2010; Lellouch et al. 2005) also result from ancient cometary impacts – our inference that Enceladus is a quantitatively viable source of Saturn's water clearly shifts the paradigm towards local or sporadic sources playing a more important role.

Nonetheless, the origin of Titan's water remains a puzzle. The scarcity of primordial noble gases in Titan's atmosphere (Niemann et al. 2010) tends to rule out cometary impacts as suppliers of volatiles there. Furthermore, based on the Landgraf et al. (2002) dust fluxes and accounting for the gravitational focusing by Saturn at Titan's distance, we have found that the micro-meteoritic flux into Titan is in the range $(0.1\text{--}0.7) \times 10^6 \text{ mol cm}^{-2} \text{ s}^{-1}$, depending on micrometeoroid velocity (i.e. their origin and orbit – interstellar, Halley-type or Kuiper Belt-like – see Moses et al. 2000). This is short of the required H₂O flux into Titan by a factor 3–80. It also remains to be understood why the IDP flux into Saturn, which is typically 16 times higher than at Titan, does not seem to deliver water there, and it may be speculated that due to their large entry velocity into Saturn ($\sim 35 \text{ km s}^{-1}$), the ablation of micrometeoroids delivers their oxygen compounds in the form of CO instead of H₂O.

References

- Bergin, E. A., Lellouch, E., Harwit, M., et al. 2000, *ApJ*, 539, L147
 Bézar, B., Lellouch, E., Strobel, D., et al. 2002, *Icarus*, 159, 95
 Bockelée-Morvan, D., & Crovisier, J. 1989, *A&A*, 216, 278
 Cassidy, T. A., & Johnson, R. E. 2010, *Icarus*, 209, 696
 Cavalié, T., Hartogh, P., Billebaud, F., et al. 2010, *A&A*, 510, A88
 Coustenis, A., Salama, A., Lellouch, E., et al. 1998, *A&A*, 336, L85
 Esposito, L. W., Colwell, J. E., Larsen, K., et al. 2005, *Science*, 307, 1251
 Farmer, A. J. 2009, *Icarus*, 149, 384
 Feuchtgruber, H., Lellouch, E., de Graauw, T., et al. 1997, *Nature*, 389, 159
 de Graauw, T., Helmich, F. P., Phillips, T. G., et al. 2010, *A&A*, 518, L6
 Hansen, C. J., Esposito, L., Stewart, A. I. F., et al. 2006, *Science*, 311, 1422
 Hansen, C. J., Esposito, L., Stewart, A. I. F., et al. 2008, *Nature*, 456, 477
 Hansen, C. J., Shemansky, D. E., et al. 2011, *GRL*, 38, L11202
 Hartogh, P., Lellouch, E., Crovisier, J., et al. 2009, *Planet. Space Sci.*, 57, 1596
 Hendrix, A., Hansen, C. J., & Holsclaw, G. M. 2010, *Icarus*, 206, 608
 Hörst, S.M., Vuitton, V., Yelle, R. V. 2008, *JGR*, 113, E10006
 Johnson, R. E., Smith, H. T., Tucker, O. J., et al. 2006, *ApJ*, 644, L137
 Jurac, S., & Richardson, J. D. 2005, *JGR*, 110, A09220
 Jurac, S., Johnson, R. E., & Richardson, J. D. 2001, *Icarus*, 149, 384
 Landgraf, M., Liou, J.-C., Zook, H. A., & Grün, E. 2002, *AJ*, 123, 8857
 Lellouch, E., Bézar, B., Moses, J. I., et al. 2002, *Icarus*, 159, 112
 Lellouch, E., Moreno, R., & Paubert, G. 2005, *A&A*, 430, L37
 Melin, H., Shemansky, D. E., & Liu, X. 2009, *Planet. Space Sci.*, 57, 1743
 Moses, J. I., Lellouch, E., Bézar, B., et al. 2000, *Icarus*, 145, 166
 Nagy, A. F., Kliore, A. K., Mendillo, M., et al. 2009. In *Saturn from Cassini-Huygens*, ed. M. K. Dougherty, et al.
 Niemann, H. B., Atreya, S. K., Demick, J. E., et al. 2010, *JGR*, 115, E12006
 Ollivier, J.-L., Dobrijevic, M., & Parisot, J.-P. 2000, *Planet. Space Sci.*, 48, 699
 Persoon, A. M., Gurmet, D. A., Santolík, O., et al. 2009, *JGR*, 114, A04211
 Perry, M. E., Teolis, B., Smith, H. T., et al. 2010, *JGR*, 115, A10206
 Pilbratt, G. L., Riedinger, J. R., Passvogel, T., et al. 2010, *A&A*, 518, L1
 Porco, C. C., Helfenstein, P., Thomas, P. C., et al. 2006, *Science*, 311, 1393
 Saur, J., Schilling, N., Neubauer, F. M., et al. 2008, *GRL*, 35, L20105
 Shemansky, D. E., Matheson, P., Hall, D. T., Hu, H.-Y., & Tripp, T. M. 1993, *Nature*, 363, 329
 Smith, H. T., Johnson, R. E., Perry, M. E., et al. 2010, *JGR*, 115, A10252
 Strobel, D. F., Atreya, S. K., Bézar, B., et al. 2009, *Atmospheric structure and composition*. In *Titan from Cassini-Huygens*, ed. R. H. Brown, et al. (Springer), 235
 Tokar, R. L., Johnson, R. E., Hill, T. W., et al. 2006, *Science*, 311, 1409
 Verbiscer, A., French, R., Showalter, M., & Helfenstein, P. 2007, *Science*, 315, 815
 Waite, J. H., Combi, M. R., Ip, W.-H., et al. 2006, *Science*, 311, 1419
 Zakharov, V., Bockelée-Morvan, D., Biver, N., Crovisier, J., & Lecacheux, A. 2007, *A&A*, 473, 303

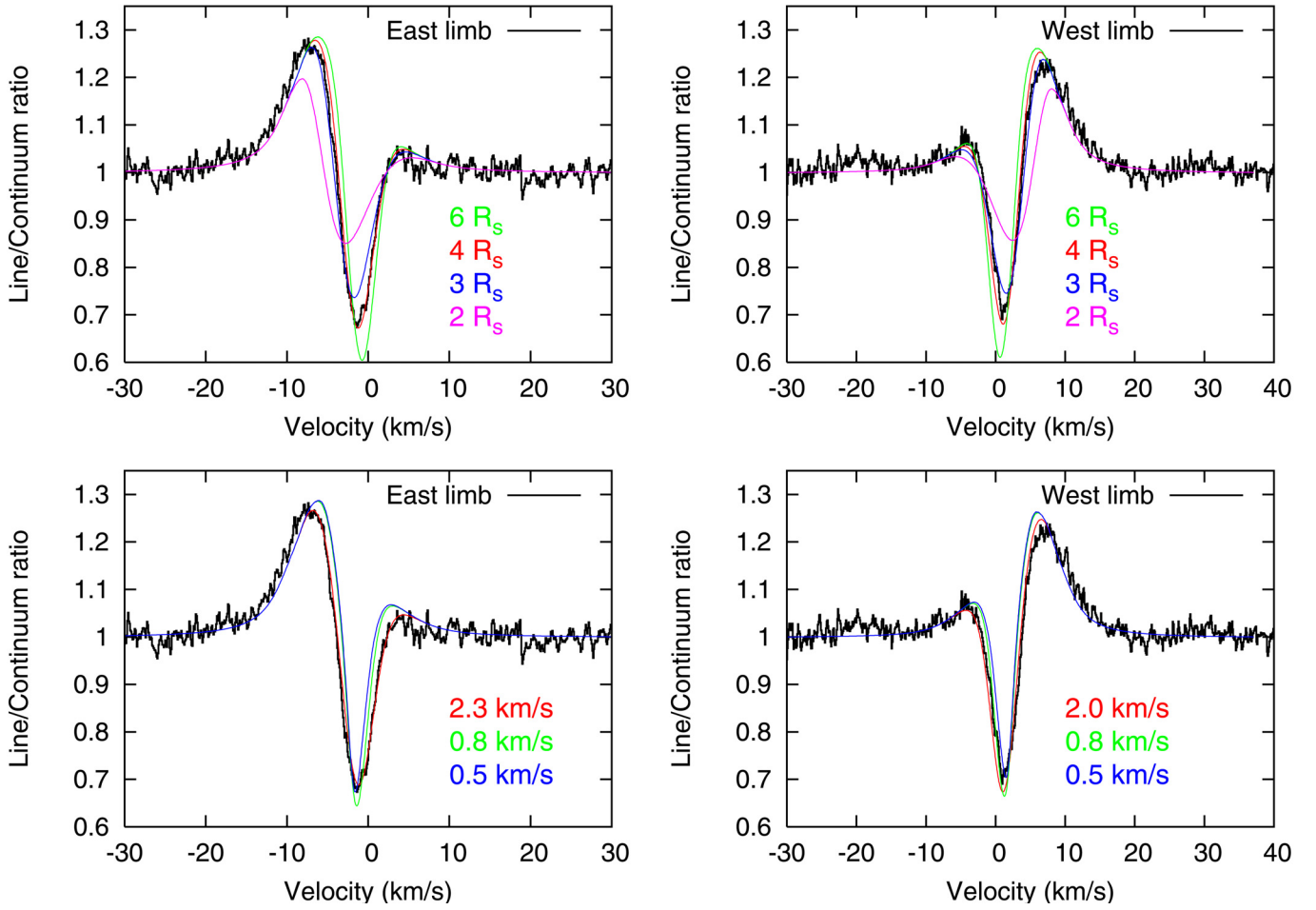


Fig. 4. Sensitivity of 1670 GHz east and west limb line profiles to (*top*) torus central position and (*bottom*) gas dispersion velocity. *Top*: model calculations, performed here for a radially infinitely narrow torus located at 2, 3, 4, and 6 Saturn radii (R_S), confirm that the absorbing material is located near $4 R_S$, and not e.g. in Saturn’s main rings at $<2 R_S$. *Bottom*: model calculations for several values of molecule dispersion velocity V_{rms} . Best fits are obtained for $V_{\text{rms}} = 2.3 \text{ km s}^{-1}$ (resp. 2.0 km s^{-1}) for the east (resp. west) limb spectrum. Dynamically colder models with $V_{\text{rms}} = 0.8 \text{ km s}^{-1}$ or $V_{\text{rms}} = 0.5 \text{ km s}^{-1}$ (typical of plume material ejection conditions) produce too narrow absorptions.

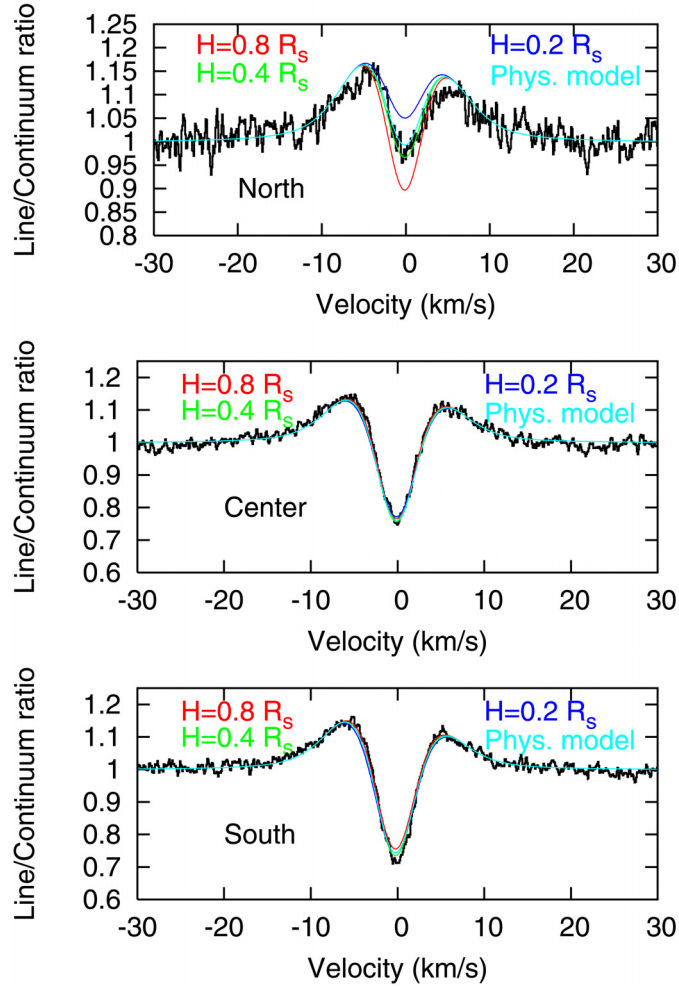


Fig. 5. Additional model fits of the 1670 GHz north, center and south observations. *Determination of the torus vertical scale height H .* Assuming that the column density falls as $N(z) = N_{\text{eq}} e^{-z/H}$, where z is the distance from the equatorial plane, the red, green, and dark blue curves correspond to $H = 0.8, 0.4,$ and $0.2 R_s$, and $N_{\text{eq}} = (2.5, 4, 8) \times 10^{13} \text{ cm}^{-2}$, respectively. The lower absorption in the northern spectrum compared to center and south indicates that $H = 0.4^{+0.2}_{-0.1} R_s$. *Test of a physical model.* The light blue curves are based on the distribution of $N_{\text{H}_2\text{O}}$ predicted from the Cassidy & Johnson (2010) model for a $0.85 \times 10^{28} \text{ s}^{-1}$ Enceladus source rate (and shown in the left panel of Fig. 3, main text). This model provides an overall good match of all H_2O lines, including the south-south asymmetry. Although not shown here, this physical model also gives a good match of the 557 and 1113 GHz absorption, and also underestimates the 987 GHz absorption by a factor ~ 1.7 .